Modeling Study of Exocytosis in Neuroendocrine Cells: Influence of the Geometrical Parameters

Javier Segura, Amparo Gil, and Bernat Soria
Instituto de Bioingeniería, Universidad Miguel Hernández, Alicante, Spain

ABSTRACT Exocytosis in neuroendocrine cells is a process triggered by Ca^{2+}. A Monte Carlo simulation of secretion has been developed which, together with the diffusion of calcium, buffered by endogenous and/or exogenously added chelators, also accounts for the dynamics of exocytosis for a pool of readily releasable vesicles. Different distributions of channels and vesicles (random or correlated) are studied. A local study of exocytosis is carried out by obtaining capacitance time courses for the different types of release-ready vesicle pools (correlated or not with Ca^{2+} channels). Also, depending upon the kinetic constants for the exocytotic process, we study the levels of local Ca^{2+} needed to trigger secretion. Our simulations show that a strong heterogeneity in the calcium concentrations at the different sites of exocytosis is a requirement for reproducing the experimentally observed biphasic response in chromaffin cells in situ (Voets, T., E. Neher, and T. Moser. 1999. *Neuron.* 23:607–615). Correlated nonuniform distributions of channels and vesicles and the existence of diffusion barriers are shown to quantitatively explain the experimental data on chromaffin cells in situ. The first description requires a deeply heterogeneous distribution, with vesicles attached to the channels or far from them, but never at middle distances. The second description is able to reproduce biphasic release even for uniformly (readily releasable) distributed vesicles. We quantify the degree of inhomogeneity in the distribution of vesicles and how porous the diffusion barriers should be to account for the observed biphasic response.

INTRODUCTION

It is widely accepted that cytosolic Ca^{2+} triggers exocytotic processes. Ca^{2+} binds to proteins present in the fusion machinery to provoke fusion of the vesicles with the plasma membrane. In neuroendocrine cells, secretion is known to be a slow process with long latencies when compared with neurotransmitter release. This fact has been explained by assuming that the spread of Ca^{2+} inside the cytosol is retarded due to the presence of endogenous buffers, together with the fact that vesicle pools are located further off the calcium channels. On the contrary, small clear granules in synapses are highly correlated to calcium channels, which explains the rapid response and short latencies observed in neurotransmitter release (see, for instance, Neher, 1998).

It was suggested by Chow et al. (1994) that calcium channels and vesicles could be randomly distributed in isolated adrenal chromaffin cells. The secretion model developed by Klingauf and Neher (1997), based on the solution of the differential equations, assumed as working hypothesis that all vesicles lie equidistantly from the channel pores and that all channel pores are equidistant among them. However, this configuration had to be refined to explain the secretion by adrenal chromaffin cells at the beginning of calcium pulses: their modeling study fitted the experimental data assuming that ~8% of vesicles are placed 30 nm from the nearest channel pore, the rest being at ~300 nm. It was then suggested that this configuration lies within the expectation for a random distribution of both channels and vesicles. However, as we will discuss, the appearance of a biphasic capacitance time course in response to a train of short depolarizations (Voets et al., 1999) in chromaffin cells in situ is difficult to explain considering uniform distributions of channels and vesicles, especially because the relative positions between channels and vesicles for random and uniform distributions should span the whole range between short and long distances.

In the case of chromaffin cells in situ it seems clear from capacitance measurements (Moser and Neher, 1997b) that there must be some degree of inhomogeneity in the distribution of calcium channels and vesicles. The secretory rates are faster than in isolated chromaffin cells in response to brief depolarizations, which suggests that the position of the vesicles shows a higher degree of correlation to the channels. Furthermore, it is observed (Voets et al., 1999) that two distinct subpools in the readily releasable pool of vesicles (RRP) can be distinguished: a pool (~35 vesicles) that depletes after few short (10-ms) depolarizations, called the immediate releasable pool (IRP), and a larger pool (~105 vesicles) insensitive to a few short pulses but sensitive to a higher number of short pulses and to larger pulses. According to Voets et al. (1999) these different subpools of the RRP are expected to arise from different geometrical arrangements. To differentiate these two distinct subpools of the RRP, we will alternatively give the name of "fast release-ready pool" (FRRP) to the IRP, while the rest of vesicles in the RRP will be called "slow release-ready pool" (SRRP). If the first subpool (~35 vesicles) is interpreted as a pool of vesicles that lies in the proximity of calcium channels while the second subpool (105 vesicles) is interpreted as consisting of vesicles more distant to the channels

Received for publication 12 January 2000 and in final form 19 June 2000.
Address reprint requests to Dr. Amparo Gil, Instituto de Bioingeniería, U.M.H, Edificio La Galia, 03202-Elche, Alicante, Spain. Tel.: 34-96-665-8411; Fax: 34-96-665-8793; E-mail: amparo.gil@umh.es.

0006-3495/00/10/1771/16 $2.00

(Voets et al., 1999), the random and uniform distribution of both channels and vesicles becomes a very improbable hypothesis. It is not possible to reconcile the appearance of two clearly distinct pools with a uniform distribution that lacks such a discontinuous behavior.

Our simulation code will allow us to study the effect on the secretory response of the geometrical configuration of both channels and vesicles. Different scenarios will be considered for the correlation between channels and vesicles, and their influence on the simulated secretion is analyzed.

It will be shown that, given the kinetic constants for endogenous and exogenous buffers (Klingauf and Neher, 1997) and for the binding of Ca^{2+} with the vesicle sensors (Heinemann et al., 1994), the more natural way to reproduce the distinct behavior of the FRRP and the SRRP, without "fine-tuning" the model, is by appropriately choosing the geometry of the distribution of channels and vesicles. Varying the rest of the parameters (binding constants and diffusion coefficients) does not prevent the model from displaying an SRRP that depletes too fast or an FRRP that depletes too slowly. Correlated nonuniform distributions of vesicles and channels and the existence of diffusion barriers are revealed as plausible explanations for the observed biphasic response. We will quantify the degree of nonuniformity in the distribution of vesicles and the extension and porosity of diffusion barriers needed to account for the observed data.

METHODS

The simulation code used in the present study is an extension of the program developed by the authors (Gil et al., 2000). The Monte Carlo code for the simulation of 3-D Ca^{2+} buffered diffusion is enhanced by incorporating the kinetics for vesicle fusion, which is also modeled as a stochastic process. The random-walk algorithm to simulate 3-D diffusion is also enhanced by incorporating diffusion barriers, which are simulated by forbidding those movements that would cross the barriers. We describe the main differences with respect to our previous simulation code and the specification of input parameters.

Domain of simulation and calcium influx

We have adopted a conical domain of 1 μm radius that can be used to model secretion by spherical neuroendocrine cells (Gil et al., 2000). An orthogonal grid covers the conical domain. The length of the grid can be varied depending on the demanded spatial resolution. For the present study, two different grid lengths ($\Delta x = 100$ nm and $\Delta x = 50$ nm) will be considered. The number of compartments in the whole conical domain is, of course, determined by the resolution of the grid. The position of the calcium pores is selected randomly and uniformly among the compartments in the upper slice (membrane) of the conical domain.

A spherical cell in which the calcium channels are uniformly distributed over the cell membrane and with a uniform distribution of calcium buffers would display an exact spherical symmetry. In this case, a conical domain reaching the center of the cell with reflecting boundaries is an accurate description. Reflection in the lateral side of the cone is interpreted as a condition of zero flux, while reflection in the upper side of the conical domain would represent real reflection of ions and buffers at the membrane. For such an ideal configuration, the relation between whole-cell current (I_{wc}) and the current entering through the upper side of the conical domain (which we will call domain current, I_d) would be given by $\beta = I_d/I_{wc} = (r/2R)^2$, r being the radius of the base of the cone and R the radius of the cell.

The approximation of a conical domain with zero flux on the lateral sides can also be safely used for smoothly nonuniform configurations in which the conical domain is placed inside a region where the distribution of channels is sufficiently uniform. In the case of a cell showing a certain degree of polarity (like chromaffin cells, Naraghi et al., 1998) one would expect a higher ratio β if the domain is inside the region of high calcium influx. A conical domain with a depth smaller than R would be then more appropriate, which also leads to a higher ratio β. In our simulations we take $R = 5$ μm, which gives $\beta = 1/100$. For a perfectly symmetric chromaffin cell of radius $R \simeq 7.5$ μm (Klingauf and Neher, 1997), $\beta_{symm} = \beta/2.25$.

Notice that, given that the relation between I_d and I_{wc} depends on the degree of the polarization of the cell, there is a relative freedom in the selection of I_d for a given whole-cell current. We will always use I_d to describe the calcium influx.

We adopt a simple model for calcium influx in which the calcium current through each pore is constant during a pulse. As discussed in Klingauf and Neher (1997), channel flickering is not relevant in order to study secretion in chromaffin cells, given the low-pass properties of the calcium sensor that controls exocytosis.

Free diffusion and diffusion barriers

The 3-D diffusion of calcium ions and buffer molecules is modeled as a random walk process (Gil et al., 2000). Calcium ions are allowed to move after each time interval $\Delta t = (\Delta x)^2/4D$, D being the diffusion coefficient, with different probabilities depending on the direction of movement (oblique moves, straight move, no movement). Mobile buffers are treated in a similar way (Gil et al., 2000).

The algorithm for free diffusion can be modified to account for diffusion barriers. A completely reflecting diffusion barrier separating two compartments of the grid can be simulated by forbidding those movements, which directly connect such two compartments. A porous barrier could also be simulated by assigning a probability for the particles of hopping through the barrier.

There is considerable freedom in the selection of the shape, location, and height of these barriers, of course limited by the finite spatial resolution. The highest resolution considered in the present study is 50 nm.

Kinetics of buffers and vesicles

Given the typical numbers of readily releasable vesicles ($\sim$100, according to Neher and Marty, 1982, and Voets et al., 1999) a discrete modeling, in which the fate of each individual vesicle is recorded, seems appropriate.

We adopt a noncooperative kinetic scheme in which three calcium ions have to bind to a protein to achieve vesicle fusion (Klingauf and Neher, 1997). This mechanism is simulated by placing three binding sides, initially free, with the kinetic constants given in Heinemann et al., 1994 (see Fig. 1) in each of the submembrane compartments where such a protein lies. The same compartment could correspond both to a channel pore and to a vesicle; in this case the vesicle would be located at a mean distance of $\sim$50 nm (for $\Delta x = 100$ nm) or $\sim$25 nm (for $\Delta x = 50$ nm) from the nearest channel.

The kinetics for binding of calcium ions to binding sites is described by first-order kinetic equations, both for the binding to buffers and to the calcium sensor of the vesicles. These kinetic equations are interpreted in a probabilistic way, as described in Gil et al., 2000. The modeling of buffers and calcium sensors differs in their different spatial distributions: the binding sites of the fusion machinery are located only where the vesicles are, while the binding sites for the buffers are randomly and uniformly distributed over the whole domain at the start of the simulations, except when explicitly stated otherwise. The last (third) binding step to the

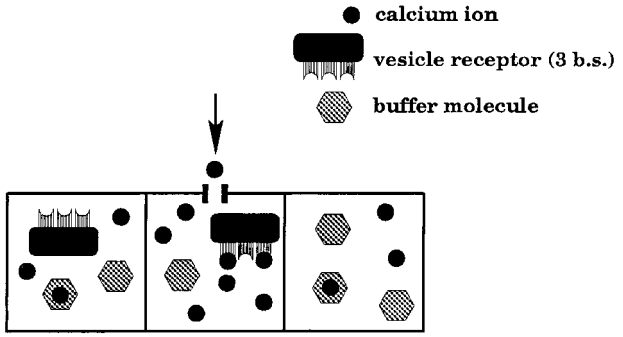

FIGURE 1 Modeling of the secretory vesicles: three binding sites (b.s.) are used to simulate the calcium sensor. These three b.s. groups are distributed among the compartments of the first slice of the conical domain.

calcium sensor is irreversible if one assumes that vesicle fusion is instantaneous after this last binding step. However, a delay time for fusion (~1 ms) is considered to account for the observed delay in secretion by neuroendocrine cells (Klingauf and Neher, 1997).

Replenishment of the RRP is not considered in this model. We will restrict our field of study to trains of pulses in the subsecond range. Endocytosis and the mobilization of additional vesicles can then be thought to be too slow to be noticed.

In summary, in our discrete description, vesicles can be understood as "calcium markers" that give information on the calcium levels reached at the site where a fusion process takes place. Describing the pace of each individual vesicle has the advantage of being able to obtain the secretory response at different positions with respect to the calcium channels in a same simulation. Therefore, we have the possibility of studying secretion time courses for different arrangements of channels and vesicles (not necessarily regularly distributed).

Finite size effects and diffusion barriers

We neglect the finite size of the vesicles in the RRP and their possible effect as calcium barriers: we simulate the kinetics for vesicle fusion but we do not consider the fact that calcium ions and buffer molecules are not free to diffuse through the space occupied by the vesicles of the RRP. This is justified given the small number of vesicles that constitutes the RRP: if vesicles were uniformly distributed we would expect one or two vesicles of the RRP in the portion of the membrane radius of 1 μm (for a total of 140 vesicles). However, the RRP is a small subpool of a larger population of vesicles (around 4000 vesicles seem "kinetically connected" for time scales of the order of ~1 min; Voets et al., 1999). Our simulations will span time intervals well below a second, for which the emergence of newly recruited and docked vesicles from reserve pools will be marginal (Voets et al., 1999); however, the existence of such vesicle pools (much larger in number than the RRP) can passively influence the response of the RRP by acting as diffusion barriers. Besides, if vesicle drift toward the membrane is stimulated by calcium, one would expect that such obstructive effects could be more important in regions of the membrane domain where the incoming Ca^{2+} flux is higher and exocytosis is faster (Robinson et al., 1995).

Later, we will discuss a modification of the simulation to account for diffusion obstacles. We will discuss how these diffusion barriers help in producing a biphasic response in secretion. However, we will first describe how to deal with the more simple situation of free buffered diffusion, and which are the outputs of such simulations.

A soft homogeneity approximation

Given that the RRP is formed only by ~100–200 vesicles, corresponding to 1–2 vesicles in our conical domain, the straightforward implementation of such distributions, though possible, is very time-consuming. We would need to run ~100 simulations to get a response for the whole RRP. Instead, we are considering an excess of vesicles in the submembrane region of the conical domain to have more significant statistics.

We have checked that, neglecting finite size effects of the vesicles in the RRP, the behavior of $k \times N$ vesicles in the conical domain is equivalent to the sum of the effects of k simulations with N vesicles each, provided the channels are distributed in a similar but not necessarily identical way in all the simulations. This approximation, consisting of placing an excess of vesicles, is expected to be sufficient for our purposes both from a geometrical and a kinetic point of view.

Regarding the geometry of the problem, the "excess of vesicles approximation" will be valid if the distribution of calcium channels is approximately uniform over the whole membrane surface. On the contrary, if the calcium channel surface density dropped and raised significantly over distances of the order of the size of our submembrane domain (radius 1 μm), we could not consider that such a membrane patch would be representative of the global distribution of channels. However, this heterogeneity would have consequences contradicting experimental data: domains of the order of 1 μm of radius or larger of high calcium concentrations and similar domains of low concentrations would be visible in fluorescence experiments. However, the distribution of calcium influx through the cell membrane in chromaffin cells does not show such broad calcium domains (Naraghi et al., 1998), but only a soft degree of polarity that is related with the position of the nucleus. Then, we can consider that a patch of 1 μm radius can be representative of the overall distribution of calcium channels. However, we check in all cases that this is so by comparing each of our results with at least two or three simulations in which the distribution of calcium channels is built by a same algorithm, but with different random seeds. These different simulations use different random distributions with similar statistical parameters (mean interchannel distance, variance of the interchannel distance, etc.) but they differ in the actual location of the channels.

With respect to the kinetic justification of the excess of vesicles approximation, given that the kinetics for exocytosis is much slower than the kinetics of endogenous and exogenous buffers and that there are many fewer binding sites in the fusion machinery than for the rest of endogenous or exogenous chelators, the binding of calcium by the exocytotic machinery is expected to affect the time course of calcium very little. This fact also explains why exocytosis can be modeled as an "a posteriori process" (as previous models do, see Klingauf and Neher, 1997): once the calcium time courses are obtained, the secretion model can, a posteriori, use this time course as input. In our simulation, the actions of buffers and of the exocytotic machinery are simultaneously taking place.

The homogeneity approximation considered here can be qualified as being soft compared to previous descriptions (Klingauf and Neher, 1997). We can study in a same simulation the contribution of vesicles located at different positions of the channel pores by considering the (soft) homogeneity hypothesis just described. Of course, we are not considering the effect of the finite size of the vesicles of the RRP, for the reasons explained before.

We tested that the simulations using an excess of vesicles ($k \times N$ vesicles) show no significant deviation from the detailed simulations (k simulations with N vesicles each); specifically, we tested this approximation for $k = 10$. Therefore, we can consider that this is not an assumption of the model, but an approximation that is known to work sufficiently well.

List of assumptions

To confront the model with experiments, it is important to outline its basic assumptions and limitations. A mismatch between theory and experiment would mean that some of the assumptions could fail. Our starting assumptions are the following:

1. Free diffusion: both the calcium ions and the mobile buffer molecules diffuse freely inside the cytosol. Diffusion of a given species is described by a single effective diffusion coefficient in the cytosol;
2. Boundary conditions: a fixed conical domain of 5 μm depth and 1 μm base radius, with null lateral fluxes, is considered in all the simulations;
3. Homogeneity in the distribution of buffers: the initial (before calcium influx) distribution of calcium and free and bound buffers is uniform all along the conical domain;
4. Endogenous buffering: we consider a single endogenous buffer with the binding and unbinding rates given in Klingauf and Neher (1997). This buffer is considered to be immobile;
5. Dynamics of exocytosis: the vesicles in the RRP fuse with the membrane after the calcium sensor binds three calcium ions, with the kinetic constants from Klingauf and Neher (1997) and Heinemann et al. (1994);
6. The calcium channels and vesicles are randomly and uniformly distributed.

We could add two simplifications to this list which, as we have checked, work with sufficient accuracy: first, to attain higher statistics of vesicle fusion in a single simulation we place an excess of vesicles in the submembrane region of our conical domain (previously discussed). Second, we are not implementing channel gating in the model, though our model is capable of including such a feature in a simple way (Gil et al., 2000). For the sake of building a configuration that displays a biphasic secretory response, it is enough considering a modeling of calcium currents in which calcium enters with equal probabilities through each of the channels. The calcium sensor of the secretory vesicles, due to their relatively slow kinetics, acts as a low-pass filter and hence channel flickering does not significantly influence secretion. Later, we will discuss that it is hard to reconcile the observed biphasic response of chromaffin cells with all six assumptions listed.

The simulations assuming the six hypotheses listed will be referred to as basic simulations, to be distinguished from the simulation in which we will modify the geometry by taking into account correlated distributions of channels and vesicles and diffusion barriers. As we will soon describe, geometrical arguments are the most natural way to explain the biphasic behavior of the secretory response of chromaffin cells.

TABLE 1 Default parameters used in the simulations

Geometric parameters	
Radius	$r = 5$ μm
Length of the grid	$\Delta x = 50$ nm*
Calcium current parameters	
Incoming current	$I_d = 3, 5, 7.5$ pA*
	Trains of 10-ms pulses* delivered at 18 Hz*
Density of Ca^{2+} channels	$\rho_{cha} = 15$ μm^{-2}*
Kinetic parameters	
Calcium	
Basal concentration	$[Ca^{2+}]_0 = 0.1$ μM
Diffusion coefficient	$D_{Ca} = 220$ $\mu m^2/s$*
Vesicles	
Forward binding rate	$k_+ = 8.10^6$ M^{-1} s^{-1}*
Dissociation constant	$K_D = 13$ μM*
Endogenous Buffers	
Total concentration	$[B] = 500$ μM*
Forward binding rate	$k_+ = 5.10^8$ M^{-1} s^{-1}*
Dissociation constant	$K_D = 10$ μM*
Exogenous Buffer	
Fura-2	
Total concentration	[Fura-2] = 100 μM
Forward binding rate	$k_+ = 5.10^8$ M^{-1} s^{-1}
Dissociation constant	$K_D = 0.24$ μM
Diffusion coefficient	$D_{Fura} = 42$ $\mu m^2/s$*
EGTA	
Total concentration	[EGTA] = 400 μM
Forward binding rate	$k_+ = 1.10^7$ M^{-1} s^{-1}
Dissociation constant	$K_D = 0.15$ μM
Diffusion coefficient	$D_{EGTA} = 200$ $\mu m^2/s$
BAPTA	
Total concentration	[BAPTA] = 200 μM
Forward binding rate	$k_+ = 5.10^8$ M^{-1} s^{-1}
Dissociation constant	$K_D = 0.2$ μM
Diffusion coefficient	$D_{BAPTA} = 200$ $\mu m^2/s$*

The parameters marked with an asterisk are varied for different simulations.

RESULTS AND DISCUSSION

The general features of our basic model are discussed next. In this description, both the calcium channels and the vesicles are uniformly and randomly distributed over the base (membrane) of the conical domain. We take $\rho_{cha} = 15$ μm^{-2} for the density of calcium channels, which would give ~10,000 channels for the whole cell ($R \simeq 7.5$ μm) in case they were uniformly distributed (Klingauf and Neher, 1997). With this density, 47 calcium channels enter our conical domain. Regarding the number of vesicles, as mentioned before, we place an excess of them to obtain significant statistics in each run of the simulation. Specifically, we place 94 vesicles in the submembrane region of the conical domain (density $\rho_{ves} = 30$ μm^{-2}). By default, the rest of parameters are fixed, as in Table 1.

Our results will be given in terms of number of exocytotic events that have taken place from the start of the stimulation. With the corresponding scale factor of 1.3 fF per fused vesicle (Moser and Neher, 1997a), these cumulative graphs can be translated into capacitance time course plots.

Calcium buffering and calcium thresholds

Let us discuss the general features of our basic simulation in which both the calcium channels and the vesicles are distributed randomly. We next show several examples of simulated capacitance time courses under different buffering conditions.

In the simulation shown in Fig. 2, we considered the values (by default) $\rho_{cha} = 15$ μm^{-2} and $\rho_{ves} = 30$ μm^{-2}, and a spatial resolution of $\Delta x = 100$ nm. The channels and vesicles are randomly and uniformly distributed. A constant domain current of 2.5 pA lasting 50 ms is considered. A fixed endogenous buffer (500 μM) is taken into account in all the simulations, with the binding ratio and dissociation constants given in Table 1.

In Fig. 2 one can observe that 200 μM BAPTA is enough to almost completely block exocytosis while, on the contrary, there is a significant amount of exocytosis with 400 μM EGTA. This reflects the fact that the binding rates for BAPTA are much larger than for EGTA. The calcium

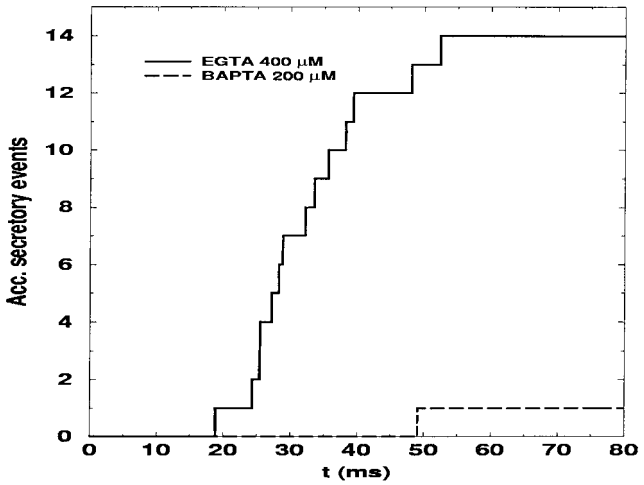

FIGURE 2 Accumulated number of vesicles that have fused to the membrane for a pool of 94 release-ready vesicles. A domain current (I_d) of 2.5 pA lasting 50 ms is considered. EGTA 400 μM (*top curve*) and BAPTA 200 μM (*bottom curve*) are chosen as exogenous buffers. The spatial resolution is $\Delta x = 100$ nm.

concentration in the submembrane domain is then much smaller for BAPTA, and the necessary calcium concentrations to trigger secretion are not reached.

By considering a current of 5 pA (Fig. 3) the situation changes drastically due to the saturation of BAPTA (Fig. 4). We see that the secretory response for BAPTA is now significant and not so different as before when we compare it with the results for 400 μM EGTA. In this case, despite a factor of ~50 of difference between the calcium binding rates for EGTA and BAPTA, the final total capacitance differs only by a factor of 2.

It has been reported by Kits et al. (1999) that in rat melanotropic cells BAPTA is only twice as effective as EGTA in blocking secretion; also, in the calyx of Held, Borst and Sakmann (1996) observed an unexpected similarity between both chelators. In Kits et al., 1999, the possibility that diffusion barriers affect the calcium transients by provoking local saturation of buffers was suggested. They found that diffusion barriers could explain the similarity between both chelators. It is also possible that the local saturation of buffers due to high local calcium currents could make the effectiveness of BAPTA and EGTA in blocking secretion more similar among them than expected from their binding ratios. By comparing Figs. 2 and 3 *A*, we observe that a moderate increase in calcium current can provoke local saturation (see Fig. 4) in such a way that the effect of both chelators approaches each other.

The binding sites of the calcium sensor are chosen to have a relatively large dissociation constant (Heinemann et al., 1994) when compared to the rates assumed for neurotransmitter release (Yamada and Zucker, 1992). This means that the calcium concentrations needed to initiate secretion in chromaffin cells and, in general, in neuroendocrine cells

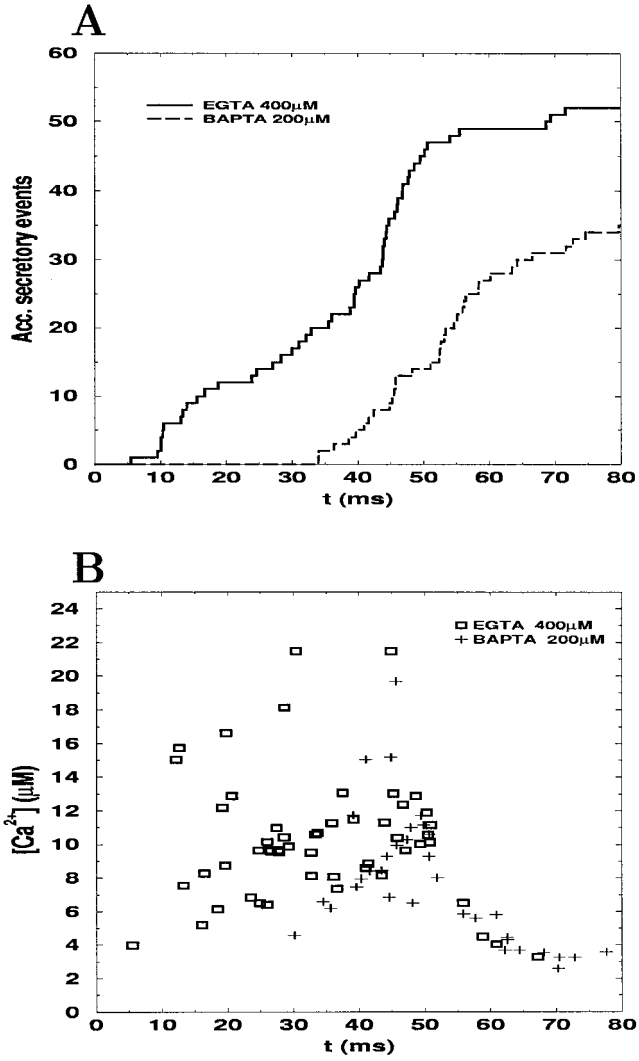

FIGURE 3 Same as Fig. 2 but for a domain current of 5 pA. EGTA 400 μM and BAPTA 200 μM are chosen as exogenous buffers. (*A*) Accumulated number of vesicles that have fused to the membrane. (*B*) Averaged Ca^{2+} levels as a function of time for each exocytotic event. The graphic shows the average calcium concentrations over the compartments of the grid that are homologous to the vesicular compartment that has suffered fusion with the membrane.

are considerably smaller than in synapses (Pertusa et al., 1999). To explore which are the calcium levels that start exocytosis, in Fig. 3 *B* we show the averaged calcium concentration reached over homologous compartments (having a vesicle) when an exocytotic event takes place. By homologous compartments we mean all those submembrane compartments that share a similar relative position with respect to the calcium channels. For instance, if a vesicle that is below a channel and without any other channel in the neighborhood suffers exocytosis, we annotate the time of this event and the calcium concentration averaged over the rest of compartments having a vesicle and lying in a homologous situation with respect to the channels. The con-

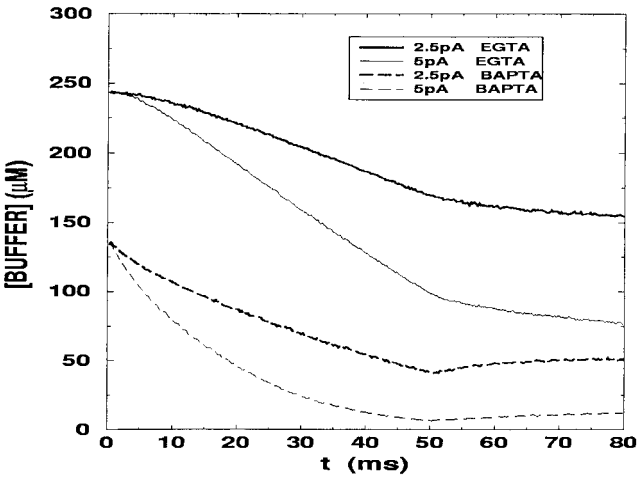

FIGURE 4 Free exogenous buffer concentration time courses under the conditions of Figs. 2 and 3. From *top* to *bottom*: EGTA 400 μM, domain current I_d = 2.5 pA; EGTA 400 μM, domain current I_d = 5 pA; BAPTA 200 μM, domain current I_d = 2.5 pA; BAPTA 200 μM, domain current I_d = 5 pA. The graph gives average concentrations on the third slice of the conical domain (depth from 200 to 300 nm). Notice that BAPTA saturates for I_d = 5 pA.

ditions in Fig. 3 *B* are the same as in Fig. 3 *A*. Let us note that most exocytotic events for EGTA added occur when the calcium concentration is higher than 6–7 μM. No event is registered for concentrations below 2 μM. The same applies for BAPTA 200 μM.

Currently, there is considerable uncertainty concerning the number of binding sites of the calcium sensor and their kinetic constants. In fact, schemes with two or four binding sites (and different kinetic constants) are also possible (Heinemann et al., 1994). We have checked (not shown) that the response obtained by other feasible sets of kinetic parameters given in the previous reference gives similar responses.

So far, the results shown stick completely to the list of assumptions previously discussed. The general features of the model, such as its dependence on the exogenous buffers, the effect of the saturation of buffers, the calcium levels needed to trigger secretion, and others not described here (see Gil et al., 2000) are qualitatively within expected.

We next confront theory with experiment to test the different hypothesis and the parameters of the model. In particular, as we describe next, the biphasic response to trains of short depolarizing pulses gives valuable information about the possible correlation of vesicles with calcium channels.

A uniform distribution of channels and vesicles fails to reproduce biphasic release

Secretion induced by depolarizing pulses often displays two distinct kinetic components (see Voets et al., 1999; Klingauf and Neher, 1997; Horrigan and Bookman, 1994, in the context of chromaffin cells): rapid (phasic) release and a sustained phase of secretion.

Previous models of secretion in chromaffin cells indicate that it is likely that several of the vesicles (FRRP) lie close to the calcium channels. In Klingauf and Neher (1997) 8% of the vesicles in the RRP were placed 30 nm from the nearest channel. It was suggested that this situation could correspond to a random distribution of both the calcium channels and the vesicles.

As Fig. 5 shows, for a density of channels $\rho_{cha} = 5\ \mu m^{-2}$ the average vesicle-channel distance is ~250 nm and ~12% of vesicles are expected to be at a distance from 0 to 100 nm to the nearest channel, corresponding to an average distance of ~50 nm. Thus, the distribution considered in Klingauf and Neher, 1997 (8% vesicles at 30 nm and 92% at 300 nm) is consistent with uniform distributions for $\rho_{cha} \simeq 5\ \mu m^{-2}$, regarding the number of vesicles that is docked near the channels. However, in a uniform scenario the distribution of vesicle-channel distances would not be so abrupt, and one could find a significant number of vesicles between 30 and 300 nm (Fig. 5).

Furthermore, the biphasic capacitance response when trains of short depolarizations are applied, both in isolated cells (Horrigan and Bookman, 1994) and in cells in adrenal slices (Voets et al., 1999), disfavors uniform distributions of channels and vesicles. Voets et al. (1999) conclude that the timing of secretion in response to the stimulation in situ by repetitive pulses and flash photolysis of caged Ca^{2+} compounds suggests that there is an FRRP of ~35 vesicles, which is a subpool of the readily releasable pool (RRP) consisting of ~140 vesicles, all vesicles being equally fusion-competent. Assuming free diffusion (no physical diffusion barriers) this would mean that the FRRP should lie in close proximity to the channels, in contrast to the rest of the RRP (which we will denote by SRRP).

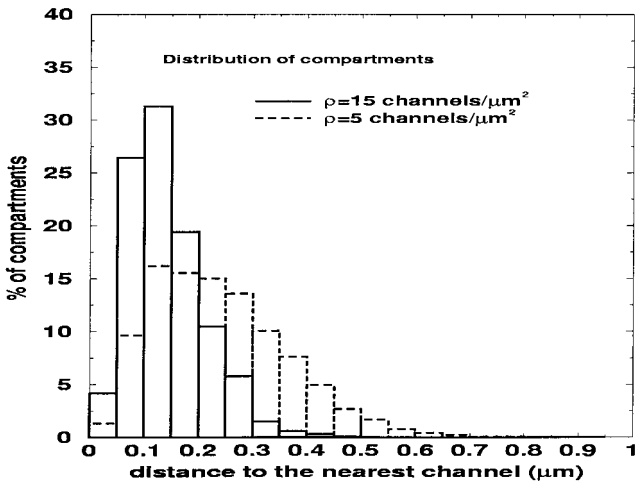

FIGURE 5 Histogram of the submembrane compartments according to the distance to the nearest calcium channel. Resolution Δx = 50 nm.

We will now study which could be the possible distribution of the FRRP and the SRRP. According to the results by Voets at al. (1999), we should look for a situation in which the FRRP may deplete due to a repetitive stimulus by short (10-ms) pulses from the very first pulse, but not the SRRP, which would start fusing with the membrane only after the first five to eight pulses.

For simulations with resolution $\Delta x = 100$ nm and random and uniform distributions of channels and vesicles, ~20% of vesicles are expected to lie inside compartments of the grid below a pore. This percentage is similar to the percentage of vesicles of the FRRP with respect to the whole RRP in chromaffin cells in situ (25%). Therefore, the FRRP could be made up by this family of vesicles. However, as we will see, when simulating these configurations, random and uniform distributions are not able to give rise to the experimentally observed biphasic release: the vesicles below a pore do not become rapidly depleted enough and therefore the FRRP is slower than it should be. Besides, the rest of the vesicles (which would constitute the SRRP) deplete too fast to be identified as a slower pool.

Fig. 6 *A* shows the capacitance time course for pulses of 10 ms separated by 45 ms, corresponding to 18 Hz (as in Voets et al., 1999). The (constant) current for each pulse is $I_d = 7.5$ pA and the channel density is $\rho_{cha} = 15\ \mu m^{-2}$. As previously, 94 vesicles are considered, which are distributed randomly and uniformly over the membrane (as well as the calcium channels). The vesicles in a compartment below a pore are supposed to form the FRRP (18 vesicles in the simulation shown, Fig. 6) while those who are not so close to the calcium channels form the SRRP (76 vesicles). One observes that the FRRP suffers depletion from the third pulse on; however, it appears strongly facilitated for the first two pulses, differently from the experimental situation, in which a dual pulse (10 ms) protocol depletes the FRRP. Besides, the SRRP is also fusing to the membrane so fast that after the fifth pulse the whole RRP has been depleted; let us observe that the fusion of the SRRP is clearly facilitated for the first three pulses (though it depletes at the end). Given that the SRRP size is larger than the FRRP, this effect becomes apparent when observing the total capacitance time course, which is also facilitated, contrary to experimental results (Voets et al., 1999).

Thus, given the kinetic constants of the model (Heinemann et al., 1994; Klingauf and Neher, 1997), the configuration considered is not enough to explain the secretory response of bovine chromaffin in situ, because one should expect an easily depleted FRRP and an insensitive SRRP for at least five pulses of 10 ms. Then, we should consider a variation of the cell current and/or a different distribution of channels and vesicles.

In Fig. 6 *B* we show the corresponding capacitance time course for 10-ms pulses with a frequency of 18 Hz and for an incoming current of 3 pA. The response of the SRRP is indeed delayed, however the contribution of the FRRP in the first three pulses becomes marginal and the FRRP is far from showing depletion. Higher calcium currents are disfavored: the FRRP would be more rapidly depleted, but the SRRP would also become depleted, which is not the situation we intend to describe. In between the results we have presented ($I = 7.5$ pA, $I = 3$ pA) there is a gradation in the results from depletion for both the FRRP and SRRP (7.5 pA) to facilitation for FRRP and a moderate but noticeable response for the SRRP. However, the situation in which the FRRP depletes while the SRRP is insensitive to the incoming Ca^{2+} (at least for the first five pulses) is not found.

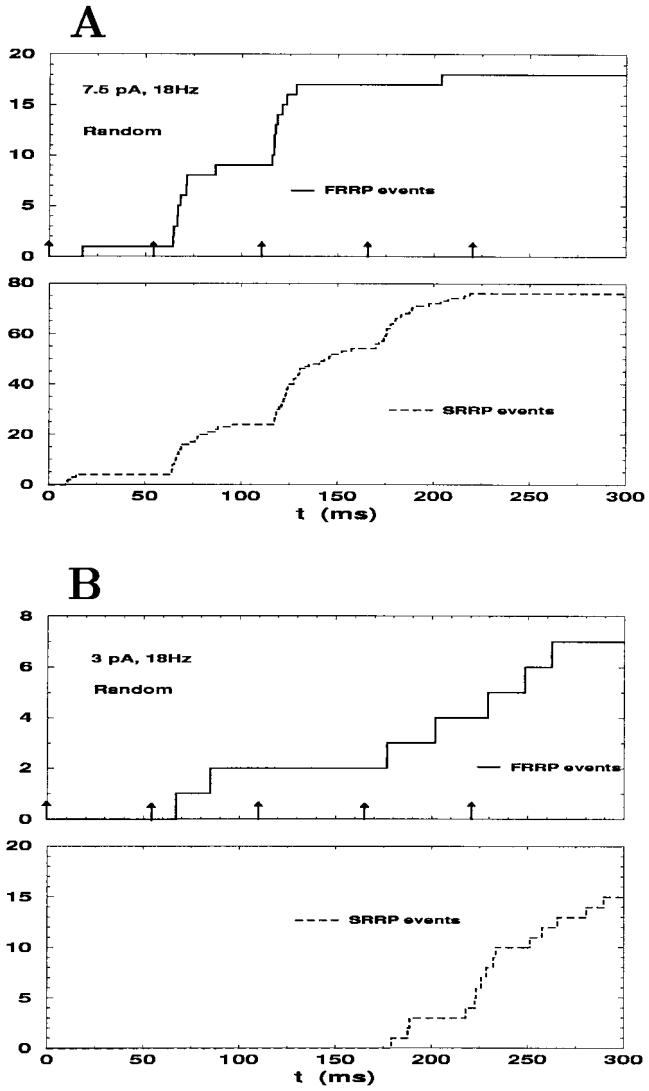

FIGURE 6 Accumulated number of vesicles that have fused to the membrane for a pool of 94 release-ready vesicles. A random distribution of vesicles is considered. The spatial resolution is $\Delta x = 100$ nm and the pulse frequency is 18 Hz. (*A*) $I_d = 7.5$ pA; (*B*) $I_d = 3$ pA.

By considering smaller channel densities for a same I_d, the FRRP will tend to deplete faster assuming that the FRRP are those vesicles below a channel. However, the ratio of

sizes of the FRRP (below a channel) to the RRP for uniform and random distributions becomes too small. Thus, random and uniform distributions of both channels and vesicles can not be accommodated with a ratio FRRP/RRP ~1:4 (Voets et al., 1999). In fact, even for $\rho_{cha} = 15\ \mu m^{-2}$ this ratio is moderately below expected (FRRP/RRP ~1:5).

Similarly, by improving the resolution ($\Delta x = 50$ nm), the FRRP could deplete faster given that the vesicles could lie closer to the channels. However, for a random and uniform distribution of vesicles the ratio FRRP/RRP becomes too small (see Fig. 5). From now on we will consider a resolution of $\Delta x = 50$ nm in our simulations. Necessarily, we must explore distributions of vesicles departing from uniformity.

Before doing this, it will be instructive to show bidimensional maps of free calcium concentrations in the submembrane domain, reached for each successive calcium pulse. This, together with the location of secretory events for a fixed random and uniform distribution of calcium channels, will guide us in how to deal with other distributions capable of giving rise to a marked biphasic release.

Submembrane calcium maps and calcium microdomains

In Fig. 7 the calcium concentrations in the submembrane domain, just before the end of each calcium pulse, are shown using pseudocolored images (*A.1–C.1*). These results correspond to a resolution $\Delta x = 50$ nm and a channel surface density of $\rho_{cha} = 8\ \mu m^{-2}$, and for three different domain currents: $I_d = 2.5$ pA (*A*), $I_d = 4$ pA (*B*), and $I_d = 7.5$ pA (*C*). As before, the calcium currents consist of 10-ms pulses at a frequency of 18 Hz. The location of each secretory event caused by each of the five pulses considered is also shown (*A.2–C.2*). The vesicles of the RRP are randomly and uniformly distributed (in the same way in all three simulations).

The distribution of calcium channels for all the plots shown (Fig. 7, *bottom left*) is also generated using a random and uniform distribution. Notice that for the particular distribution shown, groups of several channels clustered together appear. In fact, for the channel density used it is

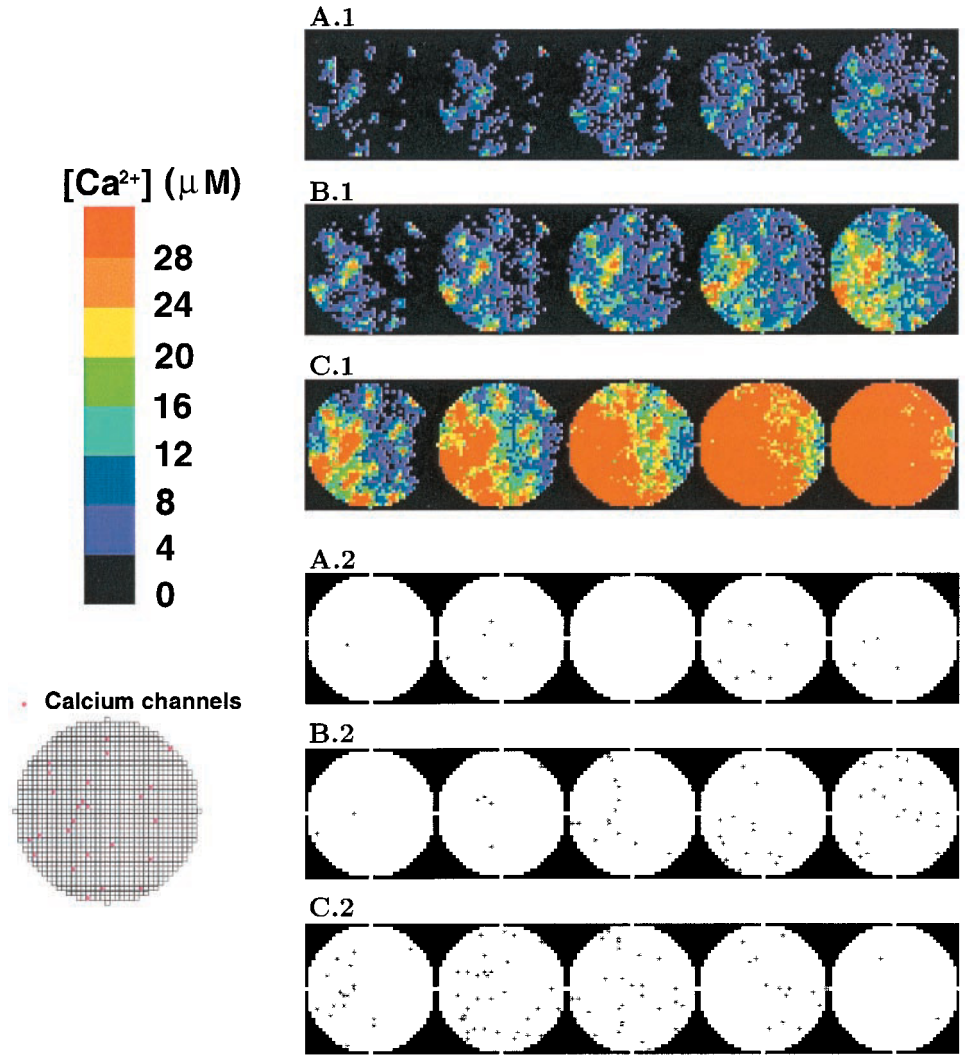

FIGURE 7 (*Top*) 2-D pseudocolored $[Ca^{2+}]$ levels plotted at the end of each 10-ms pulse for different domain currents; the images show averaged calcium concentrations over a time interval of 84 μs (30 time steps of the simulation, $\Delta x = 50$ nm): (*A.1*) $I_d = 2.5$ pA; (*B.1*) $I_d = 4$ pA; (*C.1*) $I_d = 7.5$ pA. (*Bottom*) 2-D location of secretory events caused by each pulse: (*A.2*) $I_d = 2.5$ pA; (*B.2*) $I_d = 4$ pA; (*C.2*) $I_d = 7.5$ pA.

improbable that such small clusters are not met. As seen in the pseudocolored images, these small clusters are important in determining the extension of the calcium microdomains where high enough calcium levels are reached to trigger secretion. Let us recall that, as we discussed before, the secretory events take place at locations where the calcium concentration is at least 3–4 μM. The position of these clusters determines the location of the first secretory events (*A*, *B*) unless the calcium current is so high that a single channel is capable of building a high enough calcium microdomain (*C*). For this particular distribution, calcium channels appear slightly biased toward the left of the figure, which explains the nonsymmetric calcium profiles and secretory events.

Biphasic release is not observed for any of the three currents. In the first case (*A*), the current is too low and secretory events can be considered as marginal. For 4 pA (*B*), the response is slow and secretion starts significantly from the third pulse on (no FRRP is apparent); the relative response from one pulse to the next is facilitated. Facilitation is also observed for 7.5 pA until the whole RRP starts to deplete after the third pulse. All the simulations are far from the observed biphasic release: one would need to obtain a first secretory step like the first one in Fig. 7 *C.2*, but with almost no event for the remaining four pulses. In other words, microdomains where Ca^{2+} is maintained at high enough values tend to rapidly invade the rest of the domain and provoke the fusion of the whole RRP.

In conclusion, given the kinetic constants of the model, it is not possible to explain the biphasic response in a scenario with uniformly and randomly distributed channels and vesicles. A solution to the problem may consist of a set of vesicles closely tied to the channels and a set of vesicles far away from the channels. Before exploring these and other geometrical possibilities, let us outline the possible influence of the assumptions made (listed before).

Testing the hypothesis of the model

To obtain a biphasic response resembling experiments we have to invoke different geometrical configurations. The rest of the possible modifications of the basic model (quenching of diffusion coefficients, other boundary conditions, inhomogeneity in the distribution of buffers, existence of a mobile endogenous buffer, modifications of exocytotic model) are not likely to succeed:

1. Regarding the hypothesis of free diffusion, let us consider that in the submembrane region both calcium ions and mobile buffers (mainly exogenous buffers) encounter diffuse obstacles that retard diffusion, and we can assimilate this effect to the quenching of diffusion coefficients. The net effect of diffusion is reducing the high calcium concentrations below the submembrane domain (both by the movement of Ca^{2+} ions and by the transport by mobile buffers). In this way, reducing the diffusion coefficients makes the washing out of Ca^{2+} less efficient (Gil et al., 2000) and the SRRP tends to be more sensitive to short trains of pulses. A different issue is the possibility that ions and mobile buffers may encounter walls acting as physical diffusion barriers. We cannot disregard the possibility that the SRRP consists of vesicles that are surrounded by physical barriers in such a way that Ca^{2+} must walk longer distances or cross-porous barriers before reaching the vesicles in the SRRP. We will later explore this possibility;
2. Regarding the boundary conditions imposed on the model, we have modified the conical domain but kept the rest of the parameters constant (including the domain current). For a conical domain 7.5 μm deep, similar calcium time courses are obtained in the submembrane regions, though slightly lower (differing by $<10\%$). This means that the boundary conditions imposed on the model are not critical for the evaluation of submembrane calcium concentrations;
3. With respect to the uniformity in the distribution of buffers, a possibility that seemingly could act in favor of a biphasic response is a nonuniform distribution of buffers. We performed simulations where the endogenous buffer was redistributed in such a way that it was absent in compartments below a pore and the excess of buffer was distributed among the compartments without a pore (not shown). This situation leads to higher Ca^{2+} below a pore. However, this increase in calcium concentration is not enough to significantly improve the depletion of the FRRP, given that the compartments free of endogenous buffer are surrounded by compartments with buffer which, after diffusion, tend to catch most calcium ions. Increasing the zone free of endogenous buffer creates a higher concentration of Ca^{2+}, which tends to affect the SRRP;
4. Regarding the exocytotic model, there is considerable freedom regarding the number of binding sites and the K_D for the binding of calcium. There is no reason for complicating the exocytotic model, given the experimental uncertainties. In any case, we checked that the different sets of possible parameters given in Heinemann et al., 1994, led to very similar results. Mild modifications from experimental values are not expected to alter the results in the adequate directions. For instance, lowering K_D would make the depletion of the FRRP faster, but it would influence the SRRP in a similar way;
5. We have also modified the assumption of a single immobile endogenous buffer. Following Klingauf and Neher, 1997, there are indications for a slowly moving endogenous buffer. The simulated secretory response when a single endogenous buffer is considered (with the parameters as in Table 1) compared with the same total concentration of endogenous buffer, but with a fraction (150 μM) of a mobile buffer ($D = 15$ $\mu m^2/s$), is very

similar (not shown). Although the mobile endogenous buffer acts in favor of a more insensitive SRRP (by washing out Ca^{2+} ions), its diffusion coefficient (Klingauf and Neher, 1997) is too small to have a significant effect;
6. The hypothesis of uniformity in the distribution of channels and vesicles seems difficult to reconcile with biphasic release. Next, we will consider other distributions.

The model has other intrinsic assumptions given that it is (as any model) a simplified version of a very complex system. Among the neglected effects, extrusion of calcium or uptake by internal stores could in principle have some impact on the response to trains of pulses. However, it is well known that these processes act on a larger time scale and are thus irrelevant for our simulated results (lasting ~0.3 s).

One could consider modifications of the parameters describing the basic model, however:

1. Changing the kinetics of buffers does not help. Increasing the binding reduces the depletion of the FRRP (which in our simulations does not deplete fast enough). Reducing the binding favors exocytosis by the SRRP, which in our simulations was too fast and too intense.
2. Changing the kinetics of calcium sensors in the vesicles does not help. If the calcium threshold is lowered, the SRRP will fuse earlier. On the contrary, a higher threshold would produce facilitation for the FRRP. Besides, the possible modifications of these parameters are restricted by experimental data
3. Maybe there is the possibility of fine-tuning the model by combining several of these modifications of the hypothesis and parameters. However, the more natural way to obtain a simulated response similar to experimental data consists of modifying the geometrical parameters of the model, which are the most unrestricted data in the system.

In summary, the main assumptions to be revised are the free diffusion hypothesis (by incorporating diffusion obstacles) and the assumption of uniform distributions of channels and vesicles. To these possibilities we can add the last possible ingredient that can be varied in our simulation: the shape of the calcium current. However, this ingredient will only influence vesicles that are closely tied to the channels, and therefore it is not the solution but only a possible refinement for the response of the FRRP. The SRRP is not affected by changing the shape of the calcium current (but keeping a same total current).

Our basic simulations will be modified in several ways, according to the following possibilities:

1. Calcium channels could appear clustered in small regions with a significant percentage of vesicles co-localized with the channels (FRRP). The rest of the vesicles would lie far apart from the channels;
2. Diffusion barriers can make the effective distance between channels and vesicles in the SRRP larger, and at the same time they could give rise to higher Ca^{2+} near the channels, which could deplete the FRRP faster.

Modifying the geometry: subpools of release-ready vesicles

The simulations we show next correspond to a spatial resolution of 50 nm. We consider two drastically different populations of vesicles: the FRRP will consist of those vesicles that are as close as possible to the calcium channels (at a mean distance of ~25 nm), while the SRRP will be forced to lie as far apart as possible from the channels. More specifically, we will consider that the vesicles of the SRRP are "as far as possible" from the channels when they are placed at distances higher than a given minimal distance, d_{min}; d_{min} will be chosen in such a way that the number of submembrane compartments at distances larger that d_{min} from the nearest channel will be ~10% of the total number of submembrane compartments. This is, of course, one of the more drastic situations that can be described to get two distinct phases of secretion from the same type of vesicle: we are confining the SRRP to an area that covers 10% of the submembrane domain, while the SRRP is believed to form 75% of the RRP. Fig. 8 illustrates both a random and an extreme configuration of vesicles.

First we consider a density of channels $\rho_{cha} = 15\ \mu m^{-2}$ and we distribute the 94 vesicles in the following way: 40 vesicles are forced to lie below a channel (FRRP); the rest of vesicles (SRRP) are set at least 250 nm away from the nearest channel. Fig. 5 shows that there is room enough to place the SRRP at distances larger than 250 nm. Once the uniform distribution of vesicles has been disregarded and considering our excess of vesicle approximation, the absolute values of the FRRP and the SRRP are not the relevant data of our simulations. The important thing is the relative behavior of both subpools. Thus, we will show the percentage of vesicles of each subpool that has fused with the membrane before each time. In one simulation, the size of the FRRP is limited by the number of calcium channels, while the SRRP is limited by the number of compartments at distances larger than a minimum distance (250 nm in this case). Clearly, this is not a restriction because one can average over as many simulations as needed.

Fig. 9 shows the response of the FRRP and the SRRP to short step depolarizations of 10 ms. The different behavior of the FRRP and the SRRP is more clear now than in the case of uniform distribution of both calcium channels and vesicles. Two new effects are in favor of this difference: first, given that the resolution is higher, the vesicles below a channel (FRRP) lie closer to the pores (mean distance 25 nm); second, the SRRP are more distant from the pores. For this extreme configuration and a current of 3 pA we observe (Fig. 9 *A*) that the SRRP is almost insensitive to trains of

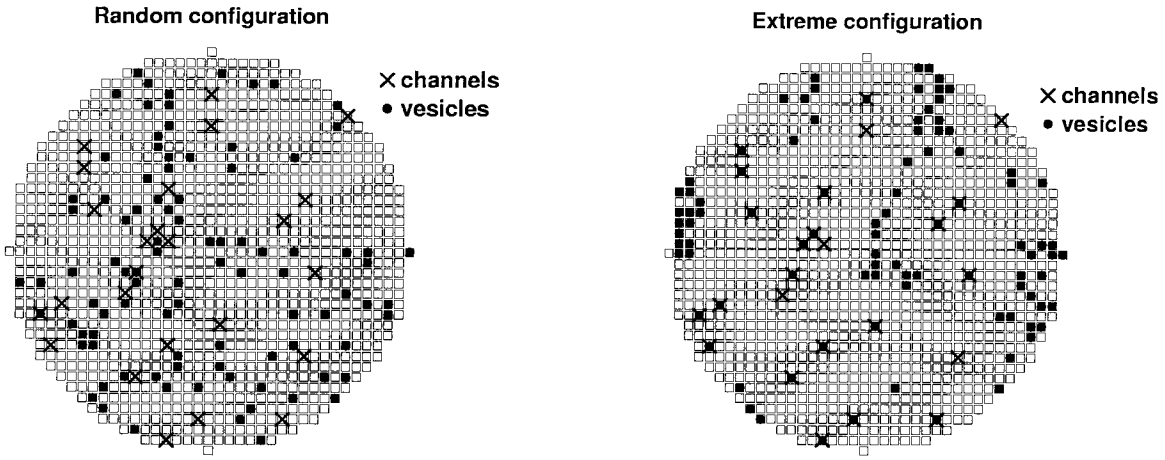

FIGURE 8 Representation of a random (*left*) and a "extreme" (*right*) distribution of vesicles.

short pulses (10 ms). Contrarily, the FRRP is seen to be half-depleted after five pulses. However, the FRRP does not completely deplete and, in fact, fusion of the FRRP is strongly facilitated for the first two pulses.

A solution to rapidly deplete the FRRP consists of increasing the domain calcium current. For a current of 7.5 pA and a density of channels $\rho_{cha} = 15\ \mu m^{-2}$ (Fig. 9 *B*), we observe that the FRRP starts to show depletion after the first 10-ms pulse. However, the counterpart is the rapid fusion of the SRRP after the second pulse, resulting in a biphasic response with a stimulation of only two short pulses.

By tuning the calcium current to middle values but keeping ρ_{cha} constant, it is not possible to reconcile a rapidly depleted FRRP with a nearly insensitive SRRP for short pulses. For instance, taking a current of 5 pA (not shown) the FRRP is not depleted rapidly enough and the SRRP remains sensitive to short pulses, and its response is retarded by only 50 ms with respect to the 7.5 pA current. Interestingly, the response with 3 pA of the SRRP was considerably different from the response for 5 pA; this is due to the saturation of Fura-2, which takes place both for 5 and 7.5 pA, but not for 3 pA (in the first five pulses). The buffering capacity of the exogenous buffer is crucial to block exocytosis by the SRRP.

Then, for a density of channels $\rho_{cha} = 15\ \mu m^{-2}$, it is difficult to accommodate the coexistence of the FRRP with the SRRP. By lowering ρ_{cha} and I_d by the same amount (thus keeping the unitary current constant), one can depress the sensitivity of the SRRP without significantly affecting the FRRP. In Fig. 10 *A* the unitary current is taken as in Fig. 9 *B*, but for a lower ρ_{cha} ($\rho_{cha} = 8\ \mu m^{-2}$). We observe that the FRRP keeps being easily depleted while the response of the SRRP is retarded ~100 ms and depressed by a factor ~2. However, the contribution of the SRRP leads to a precipitous biphasic behavior (recall the proportion of SRRP/FRRP ~3, Voets et al., 1999). Lowering ρ_{cha} again ($\rho_{cha} = 5\ \mu m^{-2}$) in Fig. 10 *B* and the domain current by the same factor (keeping then the same unitary currents), the SRRP becomes almost insensitive to the first five 10-ms pulses while the FRRP depletes, though slower than before. Fig. 10 *B* goes in the direction of a feasible solution except for the fact that the FRRP does not deplete fast enough. One can again improve the performance of the FRRP by further reducing ρ_{cha} and keeping the same I_d. Also, the shape of the calcium current can help in depleting the FRRP faster (not shown); an initial fast and intense component of the calcium current may help in depleting the FRRP without affecting the SRRP.

In any case, the most demanding experimental data are the insensitivity of the SRRP to trains of few short pulses (combined with the sensitivity of the FRRP) and, as we have discussed, this fact needs extreme geometrical configurations in a scenario of free buffered calcium diffusion. We conclude that the feasible range for the density of calcium channels or channel clusters should lie below 5 μm^{-2}, provided the SRRP is set far apart from the calcium channels. The unitary currents that rapidly deplete the FRRP are typically above 200 fA, which can represent current per calcium channel or, alternatively, current per cluster of calcium channels. It was assumed that the average distance between the vesicles in the FRRP and the channels was ~25 nm. We have checked that lowering such minimal distance to 12.5 nm (taking a grid with a spatial resolution $\Delta x = 25$ nm) does not significantly alter these ranges.

In summary, by forcing the inhomogeneity in the distribution of vesicles one can find (rather extreme) configurations that lead to biphasic release. However, though colocalization between Ca^{2+} channels and proteins of the exocytotic machinery (syntaxin, synaptotagmin, SNAP-25, etc.) has been demonstrated in neuroendocrine cells (Robinson et al., 1995; Yang et al., 1999; Wiser et al., 1999; Oheim et al., 1999), morphological studies do not suggest the existence of vesicle-free spaces between clusters of channels and vesicles. In contrast, images of densely packed

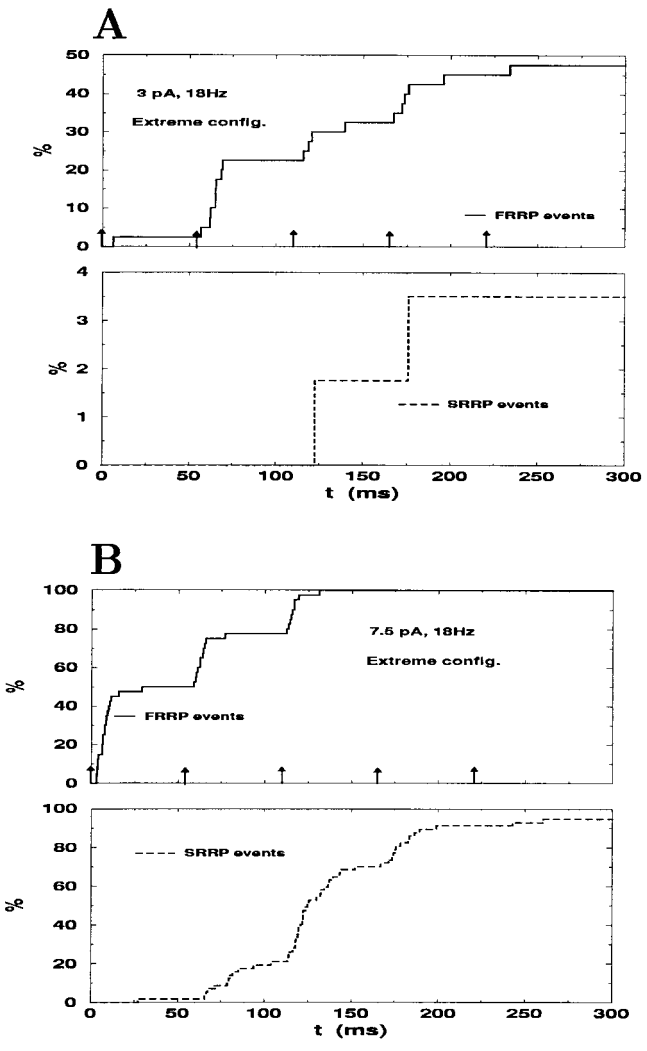

FIGURE 9 Accumulated number of vesicles (in percentage) that have fused to the membrane for a pool of 94 release-ready vesicles. We consider a resolution of 50 nm, a density of channels $\rho_{cha} = 15\ \mu m^{-2}$, and a extreme distribution of vesicles in which 40 vesicles are located below a channel pore and the rest are placed as far as possible from the channels. (*A*) I_d = 3 pA; (*B*) I_d = 7.5 pA.

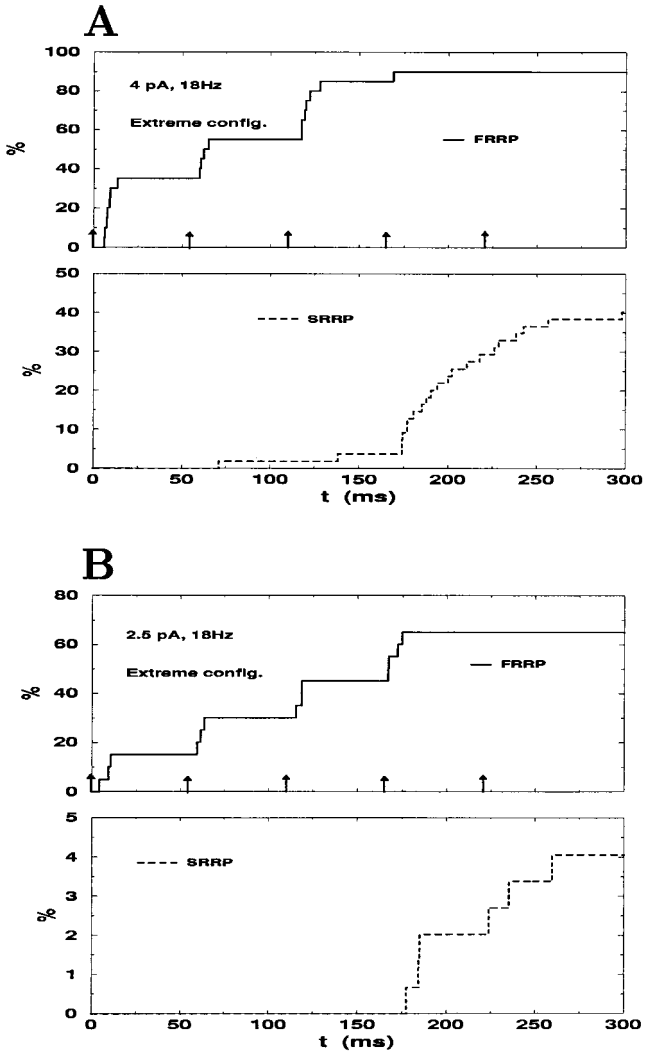

FIGURE 10 Same as Fig. 9 but for $I_d = 4$ pA, $\rho_{cha} = 8\ \mu m^{-2}$ in (*A*); and $I_d = 2.5$ pA, $\rho_{cha} = 5\ \mu m^{-2}$ in (*B*).

intracellular structures leave little free-diffusion space, which suggests that diffusion obstacles may play a role in building inhomogeneous Ca^{2+} distributions.

Effect of diffusion barriers

A further explanation for the existence of two distinct pools inside the RRP can be the presence of obstacles in the submembrane region. Diffusion obstacles were also considered by Kits et al., 1999 to explain the similarity between EGTA and BAPTA in blocking secretion, and it was discussed that the vesicles are themselves diffusion barriers that make the spread of calcium and buffers difficult. As already commented, around 4000 vesicles (Voets et al., 1999) seem to form a reserve pool that can affect the spread of calcium. One can hypothesize that vesicles tend to approach the membrane toward regions of high calcium levels (Robinson et al., 1995). In those regions, vesicles could restrict the free diffusion space that ions find after entering through the channels, and one could describe this situation by placing porous barriers around the channels. It seems reasonable that to avoid extreme distributions of vesicles, one needs highly inhomogeneous calcium profiles and to achieve this, barriers should come into play. These obstacles act in two ways: by restricting the mobility of the ions and buffer molecules near a calcium channel, the calcium concentration becomes larger near a channel. Besides, the presence of physical barriers increases the effective distance between calcium channels and the vesicles in the SRRP.

Let us consider a simple effective model in which each entry point of calcium is surrounded by a cubic porous

barrier (Fig. 11). We could interpret the FRRP as consisting of those vesicles inside the barriers, while the SRRP is formed by the vesicles outside the barriers. For the sake of simplicity, let us fix the extension of the squared diffusion barriers in such a way that by distributing the vesicles uniformly over the submembrane domain, the ratio f = FRRP/SRRP is around 0.25 (Voets et al., 1999). Then, the length of the sides of the squared base would be $l \simeq \sqrt{f/\rho_{cha}}$. The barriers are cubic, although we have checked that the depth of the barrier is not a critical parameter considering that the porosity is the same through every face of the barrier. Barriers with 100, 150, and 200 nm produced very similar results.

The porosity of the barriers will measure how densely packed the intracellular structures responsible for obstructed diffusion are. The porosity of a barrier is determined by the probability of a given ion crossing through when encountering the barrier. In our discrete simulation, a particle encounters a barrier when it tries to make a move connecting two compartments that are separated by this barrier. We consider that the barriers show the same porosity with respect to calcium ions and mobile buffers. As noted, the value of the porosity is taken to be the same through the five walls of each barrier and the barriers are considered to display the same porosity for incoming or outgoing particles.

Figs. 12 *B*, 13 *B*, and 14 *B* show the calcium time course at different distances from the channels for three different porosities: 0.01, 0.025, and 0.05. In the three cases, the upper curves correspond to calcium concentrations inside the barriers, while the rest show the calcium concentrations at different distances outside the barriers. As expected, the calcium concentrations reached inside the barriers are higher as the porosity is smaller; on the contrary, the calcium profiles outside the porous membranes are quite similar in the three cases shown. The reason for this similarity can be found in the fact that as the porosity is taken smaller, higher calcium concentrations are met inside the barriers, which increases the number of particles that encounter the

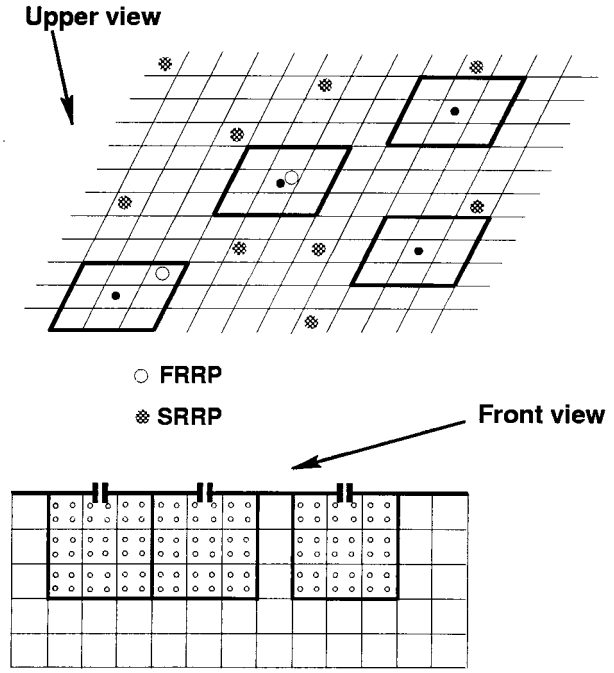

FIGURE 11 Upper and front view of the geometrical configuration for the modeling of diffusion barriers. Each channel pore is surrounded by a physical cubic porous barrier of zero width and size 150 × 150 × 150 nm^3.

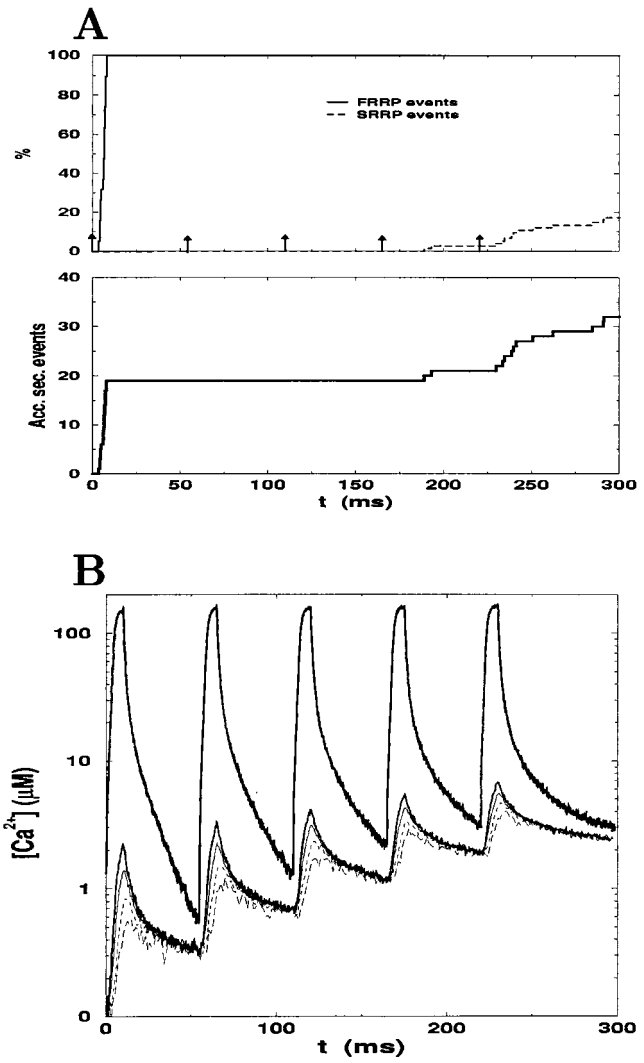

FIGURE 12 Effect of the diffusion barriers: a physical barrier of 150 × 150 × 150 nm is placed around each channel pore. A domain current of 3 pA, a density of channels $\rho_{cha} = 8\ \mu m^{-2}$, and a random distribution of vesicles are considered. The porosity of the barrier is 0.01. (*A*, *top*) Accumulated number of vesicles (in percentage) of the FRRP and SRRP that have fused with the membrane; (*bottom*) total number of accumulated secretory events. (*B*) Calcium levels at different distances from the nearest channel. From top to bottom, the curves shown correspond approximately to the following intervals of distances to the nearest channel (in nanometers): [0, 100], [100, 150], [150, 200], [300, 350], [400, 450].

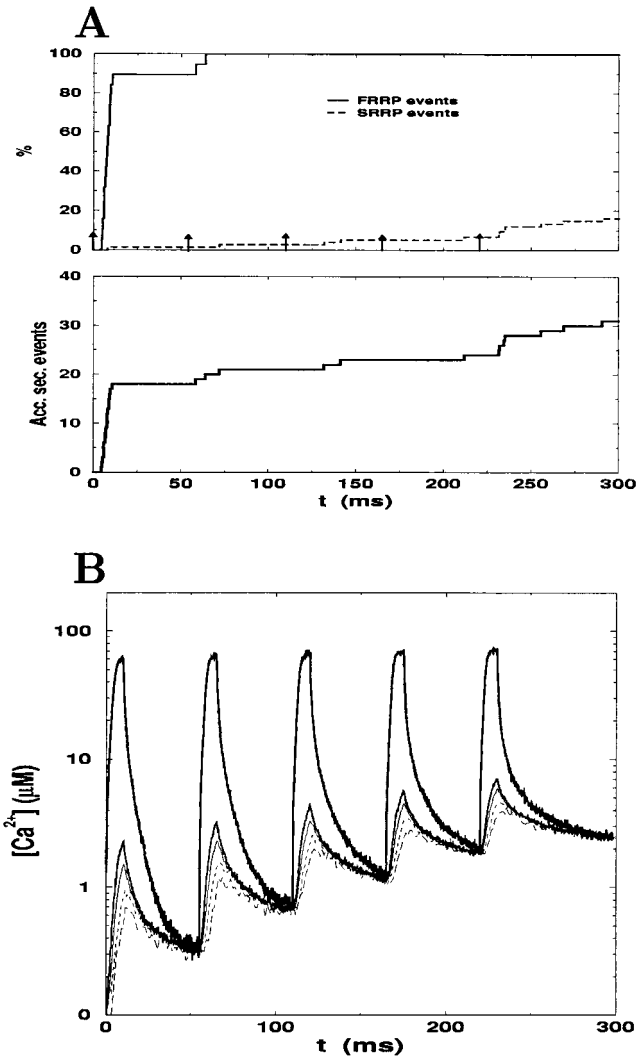

FIGURE 13 Same as Fig. 12 for a porosity of 0.025.

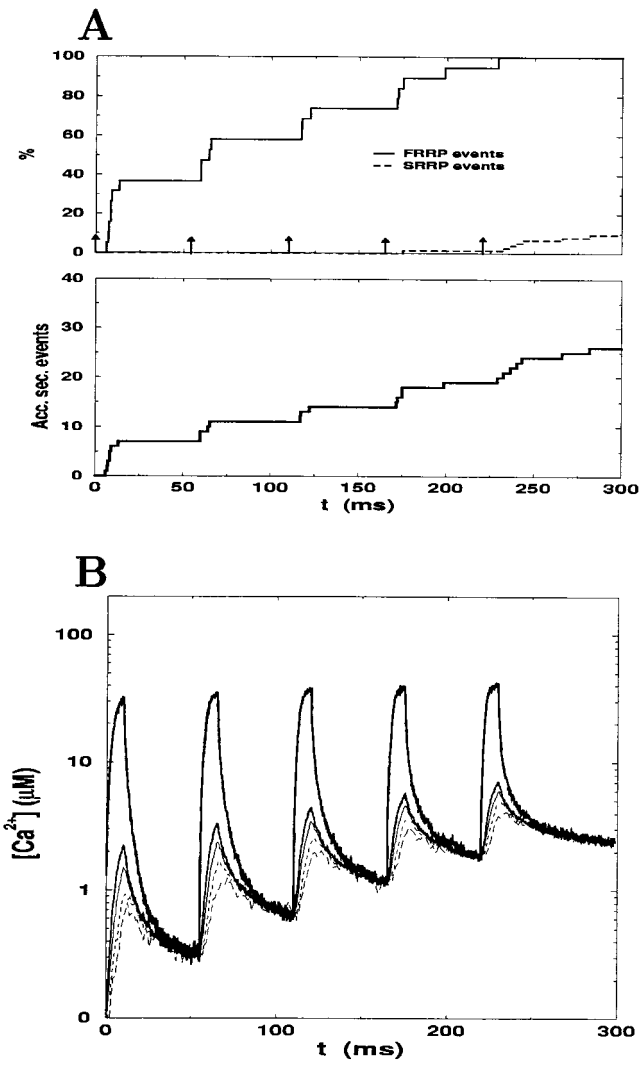

FIGURE 14 Same as Fig. 13 for a porosity of 0.05.

barrier per unit time and results in a similar net flux outward from the barriers for the different porosities.

The main effect of the porous barriers consists of increasing the calcium concentration inside them while keeping similar calcium gradients outside the barriers, which are quite similar to those obtained without barriers (not shown). These calcium microdomains inside barriers provide high calcium concentrations during calcium influx that rapidly equilibrate after the cessation of the pulse. The time of equilibration depends on the Ca^{2+} levels reached inside the barrier, ranging from ~10 ms for a porosity $p = 0.05$ (Fig. 14 *B*) to ~50 ms (Fig. 12 *B*) for $p = 0.01$. For $p = 0.025$ only experiments with a spatial resolution better than ~200 nm and a simultaneous temporal resolution better than ~30 ms would be capable of observing these transient calcium microdomains.

Given that the SRRP are supposed to be those readily releasable vesicles outside the barriers and given the soft dependence with the porosity of the calcium levels outside the barriers, the main parameter that controls the response of the SRRP is the domain current (apart from its binding constants, supposedly identical to the binding constants for the vesicles of the FRRP, following Voets et al., 1999). The calcium microdomains formed by the porous barriers may reach high enough concentrations to rapidly and completely deplete the FRRP without affecting the SRRP.

Figs. 12 *A*, 13 *A*, and 14 *A* show the accumulative percentages of FRRP and SRRP that have fused with the membrane as well as the total response as a function of time. Notice that the extension of the diffusion barriers has been fixed in such a way that the relative sizes of the FRRP and SRRP are in proportion close to the experimental data. Thus, a simulation can be considered successful if the total response (FFRP + SSRP) has a shape similar to the experiment. We choose a domain current of 3 pA, which guarantees that vesicles of the SRRP (not in the neighborhood of

a channel) will be almost unaffected by the first five pulses (10-ms pulses at 18 Hz). Both for a porosity $p = 0.01$ and for $p = 0.025$ we clearly obtain a marked biphasic response, while the porosity $p = 0.05$ tends to be slightly higher than required, since the FRRP does not deplete fast enough.

Let us stress that although calcium levels around $\sim 3\ \mu$M are able to trigger secretion, the rapid response of the FRRP requires higher levels, given that the whole FRRP should be close to depletion after the first pulse. A rough (under)estimate of the typical time needed for a secretion event to take place gives $\tau \sim 1/k_+[Ca^{2+}]$, which for the binding constant of the binding sites of the vesicle receptor gives $\tau \sim 100/[Ca^{2+}]$ ms, with $[Ca^{2+}]$ expressed in μM. Therefore, if we require that most of the vesicles of the FRRP fuse in the first 10-ms pulse we will need $\tau < 10$ ms, and therefore a calcium concentration well above 10 μM should be maintained during the pulse.

The simulated results shown in Figs. 12 and 13 are able to produce calcium levels well above 10 μM and to deplete the FRRP in the first pulse. On the contrary, the porosity for Fig. 14 is too high to allow for a high enough calcium concentration. In all three cases, the SRRP is seen to be almost unaffected for the first five pulses.

CONCLUSIONS

A comprehensive model to study secretion by neuroendocrine cells has been developed. We have confronted the model with experiments in chromaffin cells to test the basic hypothesis of the model.

The hypothesis of uniformity in the distributions of channels and vesicles failed to reproduce the observed biphasic response of chromaffin cells due to trains of short depolarizations. A reasonable solution, without fine-tuning the model, consists in reducing the channel density or, alternatively, concentrating the channels in small clusters. At the same time, we simultaneously required positive and negative correlation between channels and vesicles. In this way, twice-peaked distributions of vesicles were considered that led to a population of vesicles closely tied to the channels (FRRP) depletable by short pulses and a second population of vesicles far off the channels (SRRP) insensitive to five or six short depolarizations. By considering these "extreme" distributions of vesicles with respect to the calcium channels, we set lower bounds on the interchannel (or intercluster) distances and the local calcium currents.

Considering this description, the main question that remains opened is the mechanism by which the vesicles should either be closely tied to the channels or quite far from them, but not at middle distances. A different description, without requiring correlation between channels and vesicles, is the presence of diffusion barriers forming corrals of transient high calcium concentrations. This description is able to reproduce the observed biphasic behavior with randomly and uniformly distributed channels and vesicles.

Other modifications of the model (not geometrical) did not lead to a good compromise between theory and experiment. Thus we conclude that, given the kinetics of endogenous buffers and of the secretory machinery, geometrical arguments are the key to understanding the biphasic behavior.

We conclude that the mere redistribution of the channels and vesicles below the submembrane domain may be sufficient to explain the appearance of two distinct subpools of the RRP. However, the configuration needed tends to be extreme. The appearance of diffusion barriers helps in establishing these two distinct subpools in a more natural way.

A.G. and J.S. acknowledge the hospitality of CWI (Amsterdam) where part of this work was done.

This study was supported in part by grants from Ministerio de Educación y Cultura (PM 98-0105), European Commission (IFD97-1065-CO3-02), Fundació la Marató de TV3, and Generalitat Valenciana (GV99-146-1-04).

REFERENCES

Borst, J. G. G., and B. Sakmann. 1996. Calcium influx and transmitter release in a fast CNS synapse. *Nature.* 383:431–434.

Chow, R. H., J. Klingauf, and E. Neher. 1994. Time course of Ca^{2+} concentration triggering exocytosis in neuroendocrine cells. *Proc. Natl. Acad. Sci. U.S.A.* 91:12765–12769.

Gil, A., J. Segura, J. A. G. Pertusa, and B. Soria. 2000. Monte Carlo simulation of 3-D buffered Ca^{2+} diffusion in neuroendocrine cells. *Biophys. J.* 78:13–33.

Heinemann, C., R. H. Chow, E. Neher, and R. S. Zucker. 1994. Kinetics of the secretory response in bovine chromaffin cells following flash photolysis of caged Ca^{2+}. *Biophys. J.* 67:2546–2557.

Horrigan, F. T., and R. J. Bookman. 1994. Releasable pools and the kinetics of exocytosis in adrenal chromaffin cells. *Neuron.* 13: 1119–1129.

Kits, K. S., T. A. de Vlieger, B. W. Kooi, and H. D. Mansvelder. 1999. Diffusion barriers limit the effect of mobile calcium buffer on exocytosis of large dense cored vesicles. *Biophys. J.* 76:1693–1705.

Klingauf, J., and E. Neher. 1997. Modeling buffered Ca^{2+} diffusion near the membrane: implications for secretion in neuroendocrine cells. *Biophys. J.* 72:674–690.

Moser, T., and E. Neher. 1997a. Estimation of mean exocytotic vesicle capacitance in mouse adrenal chromaffin cells. *Proc. Natl. Acad. Sci. U.S.A.* 94:6735–6740.

Moser, T., and E. Neher. 1997b. Rapid exocytosis in single chromaffin cells recorded from mouse adrenal slices. *J. Neurosci.* 17:2314–2323.

Naraghi, M., T. H. Müller, and E. Neher. 1998. Two-dimensional determination of the cellular Ca^{2+} binding in bovine chromaffin cells. *Biophys. J.* 75:1635–1647.

Neher, E. 1998. Vesicle pools and Ca^{2+} microdomains: new tools for understanding their roles in neurotransmitter release. *Neuron.* 20: 389–399.

Neher, E., and A. Marty. 1982. Discrete changes of cell membrane capacitance observed under conditions of enhanced secretion in bovine adrenal chromaffin cells. *Proc. Natl. Acad. Sci. U.S.A.* 79:6712–6716.

Oheim, M., D. Loerke, W. Stühmer, and R. H. Chow. 1999. Multiple stimulation-dependent processes regulate the size of the releasable pool of vesicles. *Eur. Biophys. J.* 28:91–101.

Pertusa, J. A. G., J. V. Sánchez-Andrés, F. Martin, and B. Soria. 1999. Effects of calcium buffering on glucose-induced insulin release in mouse

pancreatic islets: an approximation to the calcium sensor. *J. Physiol. (Lond.).* 520:473–483.

Robinson, I. M., J. M. Finnegan, J. R. Monck, and R. M. Wightman. 1995. Colocalization of calcium entry and exocytotic release sites in adrenal chromaffin cells. *Proc. Natl. Acad. Sci. U.S.A.* 92:2474–2478.

Voets, T., E. Neher, and T. Moser. 1999. Mechanisms underlying phasic and sustained secretion in chromaffin cells from mouse adrenal slices. *Neuron.* 23:607–615.

Wiser, O., M. Trus, A. Hernández, E. Renstrom, S. Barg, P. Rorsman, and D. Atlas. 1999. The voltage sensitive Lc-type Ca^{2+} channel is functionally coupled to the exocytotic machinery. *Proc. Natl. Acad. Sci. U.S.A.* 96:248–253.

Yamada, W. M., and R. S. Zucker. 1992. Time course of transmitter release calculated from simulations of a calcium diffusion model. *Biophys. J.* 61:671–682.

Yang, S. N., O. Larsson, R. Branstrom, A. M. Bertorello, B. Leibiger, I. B. Leibiger, T. Moede, M. Kohler, B. Meister, and P. O. Berggren. 1999. Syntaxin 1 interacts with the L(D) subtype of voltage-gated Ca^{2+} channels in pancreatic beta cells. *Proc. Natl. Acad. Sci. U.S.A.* 96: 10164–10169.